doi:10.1016/j.jmb.2005.09.096 J. Mol. Biol. (2005) 354, 940–951

JMB

Available online at www.sciencedirect.com

SCIENCE DIRECT®

ELSEVIER

Crystal Structure of Wild-type Chaperonin GroEL

Cecilia Bartolucci[1]*, Doriano Lamba[2], Saulius Grazulis[3] Elena Manakova[3] and Hermann Heumann[4]

[1]*Istituto di Cristallografia CNR, P.O. Box 10, I-00016 Monterotondo Stazione Roma, Italy*

[2]*Istituto di Cristallografia CNR, Area Science Park Basovizza, S.S.14 Km 163.5 I-34012 Trieste, Italy*

[3]*Institute of Biotechnology Graciuno 8, LT-02241 Vilnius Lithuania*

[4]*Max-Planck Institut für Biochemie, Abteilung Membran und Neurophysik, Am Klopferspitz 18, D-82152 Martinsried bei München Germany*

**Corresponding author*

The 2.9 Å resolution crystal structure of apo wild-type GroEL was determined for the first time and represents the reference structure, facilitating the study of structural and functional differences observed in GroEL variants. Until now the crystal structure of the mutant Arg13Gly, Ala126Val GroEL was used for this purpose. We show that, due to the mutations as well as to the presence of a crystallographic symmetry, the ring–ring interface was inaccurately described. Analysis of the present structure allowed the definition of structural elements at this interface, essential for understanding the inter-ring allosteric signal transmission. We also show unambiguously that there is no ATP-induced 102° rotation of the apical domain helix I around its helical axis, as previously assumed in the crystal structure of the $(GroEL\text{-}KMgATP)_{14}$ complex, and analyze the apical domain movements. These results enabled us to compare our structure with other GroEL crystal structures already published, allowing us to suggest a new route through which the allosteric signal for negative cooperativity propagates within the molecule. The proposed mechanism, supported by known mutagenesis data, underlines the importance of the switching of salt bridges.

© 2005 Elsevier Ltd. All rights reserved.

Keywords: allostery; cooperativity; chaperonins; GroEL; crystal structure

Introduction

The GroEL chaperonin system, responsible for the folding of a wide variety of unrelated proteins, consists of 14 identical subunits assembled in two heptameric rings stacked back to back exhibiting *D*7*2* symmetry. Each subunit is composed of an apical domain (residues 189–377) that binds non-folded proteins and GroES, an intermediate domain (residues 137–188 and 378–409), and an equatorial domain (residues 2–136 and 410–525) that binds ATP and is involved in inter-ring interactions. The two rings alternate their role as a polypeptide-accepting and -folding chamber in a cycle triggered by ATP binding. Also necessary to the folding cycle is the co-chaperonin GroES, whose binding to the ATP-bound ring induces major conformational changes in the apical and intermediate domains.[1–3]

This large macromolecular assembly is a highly allosteric system showing positive cooperative binding of ATP by the subunits within one ring and negative cooperativity with respect to ATP binding by the subunits in the opposite ring.[4] Positive cooperativity leads to concerted binding and release of GroES and substrate proteins, whereas negative cooperativity results in asymmetric complexes with the two rings adopting different conformations. This is characteristic of the operating mode of this chaperonin system, which requires the alternating functioning of each ring in a piston-like fashion, possible only if communication between the two rings is maintained throughout all stages of the cycle by means of interactions across the ring–ring interface. Studies of the mechanism of negative cooperativity based on structural analysis led to the belief initially that it was due mainly to steric clashes and that allosteric effects were transmitted across the rings primarily through *en bloc* movements rather than conformational changes within the domains.[5,6] However, kinetic as well as structural studies of mutants with altered cooperativity are not in line with this view.[7,8]

Here we report the crystal structure of the wild-type non-bound GroEL protein (apo-GroEL), which can be considered the "zero state" since it is the state in which the protein is found prior to entering

Abbreviations used: DM, double mutant; NCS, non-crystallographic symmetry; PDB, Protein Data Bank.

E-mail address of the corresponding author: cecilia.bartolucci@ic.cnr.it

0022-2836/$ - see front matter © 2005 Elsevier Ltd. All rights reserved.

the GroEL cycle. It should be regarded as reference in the comparison with other known GroEL structures allowing us to portray better structural flexibility in the GroEL subunits. The only previously available crystal structure of the apo-GroEL protein[9] (Protein Data Bank (PDB) code: 1OEL) had two important limitations: (i) it showed a strict crystallographic 2-fold symmetry between the protomers in the two rings, preventing the study of the functional ring–ring interface; (ii) it contained two point mutations, one of which, the mutation Arg13Gly, greatly affects negative cooperativity.[7] In fact this double mutant (DM) of GroEL Arg13Gly, Ala126Val is viable *in vivo* and *in vitro*,[4] but shows altered ATPase activity and allosteric transitions compared to wild-type GroEL. It has also been proposed that the Arg13Gly mutation, since it disrupts inter-ring communication, is responsible for ATP to be bound in both rings in the crystal structure of the DM-GroEL(ATP)$_{14}$ (PDB code: 1KP8),[10] and is ultimately responsible for the lack of asymmetry between the rings, resulting in a state that is not present in the GroEL cycle.

Here, special attention has been given to the analysis of the ring–ring interface, the helix I and the mobility of the apical domains. Furthermore the comparison of our structure with two others previously elucidated, the DM-GroEL(ATP)$_{14}$[10] and the GroEL-GroES-(ADP)$_7$,[3,5] (PDB code: 1PF9) allowed us to envisage a new route for the transmission of the allosteric signal.

Results

Crystal structure

Crystals of wild-type GroEL belong to the orthorhombic space group $P2_12_12_1$ with one molecule (14 subunits) in the crystallographic asymmetric unit. The application of non-crystallographic symmetry (NCS) restraints with differentiated weights for the three domains of each subunit (see Materials and Methods), enabled us to provide an adequate conformational degree of freedom within each of the subunits, without leading to over-fitting of the model.[11] A stretch of residues encompassing Val29-Pro34, was released from NCS restraints during the last cycles of refinement so as to determine freely the conformation of the main-chain carbonyl of Leu31, which plays an important role in the propagation of the allosteric signal as a consequence of ATP binding. In addition a composite omit σ_a-weighted ($2F_o-F_c$, ϕ_c) electron density map was calculated. This procedure clearly showed that the carbonyl moiety in the Leu31-Gly32 peptide bond can easily flip. In the present apo structure it was found both in the *cis* (nine times) and in the *trans* conformation (five times) being respectively engaged or not in hydrogen bonding with $N^{\delta 2}$ of Asn457 (Figure 1).

A strong electron density visible in the region between Leu31 and Lys51 suggested the presence of an ion, which we assumed to be K^+, as in two other GroEL structures[3,10] also considering that K^+ is required for ATPase activity.[12]

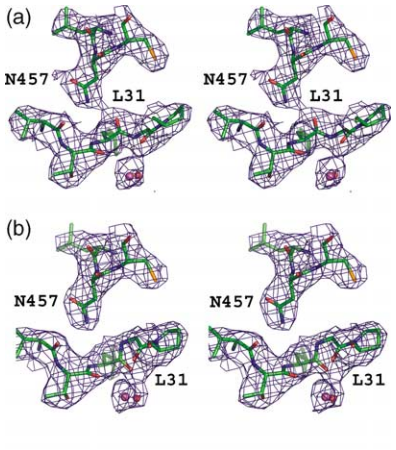

Figure 1. Stereo $2F_o-F_c$ density composite omit map of the region around Leu31. (a) *Cis* conformation of Leu31 main-chain carbonyl. (b) *Trans* conformation. The maps are contoured at 1σ.

Inter-ring contacts

The present structure is the first apo-GroEL structure, which allows the examination of the ring–ring interactions. Each subunit interacts at the ring–ring interface with a 1:2 subunit stochiometry showing two regions of contact, termed right and left.[9] Careful analysis of these contacts confirmed what had previously been observed in the study of the interface of the DM-apo-GroEL structure[11] modelled by applying the crystallographic 2-fold symmetry: there are surprisingly few hydrogen bonds stabilizing the association between the two rings. In fact the only major inter-ring interaction is the salt-bridge between Arg452 and Glu461 at the right site. A salt-bridge at the left site between Lys105 and Glu434 has been reported in several EM studies[8,13,14] and its role analyzed by site-directed mutagenesis.[15] However, in our, as well as in all other crystal structures, no interaction between Lys105 and Glu434 can be seen. Calculation of SA-omit maps around residues Lys105 and Glu434 showed a well-defined density around Lys105 side-chain in all 14 subunits, while this is not the case around Glu434. However, Lys105 is engaged in a salt-bridge with Glu102 belonging to the same subunit with an average distance of 3.1 Å. The same interaction can also be found in the ADP-bound asymmetric GroEL-GroES structure of wild-type GroEL.[3,5]

The importance of the inter-ring interaction between Arg452 and Glu461 has been further confirmed in a recent study on the GroEL Glu461Lys mutant.[13] The cryo-EM structure at 24.5 Å resolution shows a reorganization of

the ring–ring interface in which each subunit interacts with only one subunit of the opposite ring, shifting the stochiometry from 1:2, as in the wild-type structure, to 1:1.

Rotation of helix I

It has been assumed,[10] that upon binding of ATP, the apical domain surface helix I (residues 257–268) undergoes a rotation of 102° around its helical axis, causing a large lateral displacement of the apical domain surface and a significant reduction of its hydrophobic property. When comparing the DM-GroEL(ATP)$_{14}$ structure with the apo-DM-GroEL structure,[9] this rotation gives rise to a deceptive superposition, since there is an almost perfect shift of register of one amino acid. However in the asymmetric GroEL-GroES-(ADP)$_7$ structure[3,5] (GroEL-GroES-(ADP)$_7$, PDB accession code: 1PF9) there is no difference in the rotation of helix I in the ADP-bound and ADP-free ring, which is the same as the one found in the DM-GroEL(ATP)$_{14}$ structure.[10]

In order to establish unambiguously the rotation of helix I, we refined the wild-type apo-GroEL structure twice, applying exactly the same protocol,[11] while using two different models, 1OEL[9] and 1KP8,[10] which display the two different rotations. We calculated in both cases a composite omit σ_a-weighted ($2F_o-F_c$, ϕ_c) electron density map around helix I (residues 254–269). The results clearly indicate that the only correct interpretation of helix I rotation corresponds to that found in the DM-GroEL(ATP)$_{14}$ structure, showing that the rotation of this structural element is independent of the nucleotide binding (Figure 2).

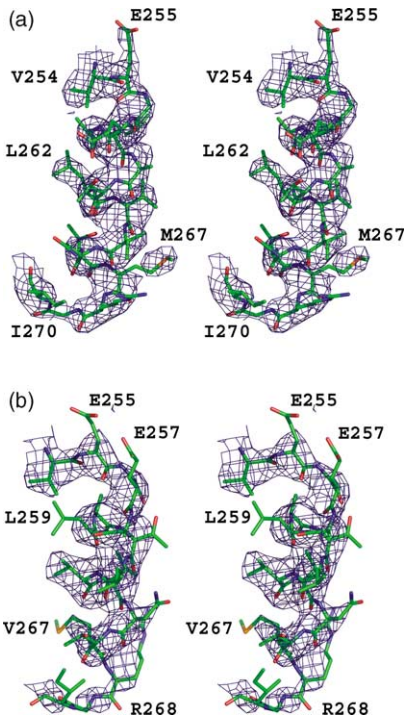

Figure 2. Stereo diagram of $2F_o-F_c$ density composite omit maps of helix I (a) shows well-defined electron density obtained using 1KP8 as model. Electron density for (b) was obtained using 1OEL as model. The maps are contoured at 1σ.

Mobility of the apical domains

Deviations from the *D7* non-crystallographic symmetry result in geometrical as well as dynamic differences among the single subunits within the oligomer. These differences are greater among the apical domains, confirming the higher flexibility ascribed to this part of the molecule, necessary for the binding of different protein substrates.

Extensive rebuilding and accurately weighted NCS restraints allowed us to evaluate the mobility of the domains within one oligomer. We followed the approach used in the analysis of the DM-GroEL(ATP)$_{14}$[10] and DM-GroEL(peptide)$_{14}$ (PDB code: 1MNF)[16] structures. In order to obtain an averaged subunit conformation in each of the three states, independent subunits were simultaneously superimposed using C^{α} coordinates of the equatorial domain residues, and the resulting coordinates were averaged. Domain motion angles were then deduced from these averaged subunit conformations.

Superimposition of all subunits using the equatorial domains of the apo-GroEL structure showed conformational variations with a rotational spread of 12.3° at the apical domains (Figure 3(a)). The maximal rotation angles in the DM-GroEL(ATP)$_{14}$ and DM-GroEL(peptide)$_{14}$ structures are 7.4° and 2.1°, respectively. These values indicate that inter-subunit domain–domain interactions are enhanced by ATP, and even more by peptide binding.

Superimposition of the averaged coordinates of the three structures (Figure 3(b) and (c)), shows a greater movement of the apical domain of the ATP-bound structure compared to the peptide-bound one. This is in agreement with the small movement reported by Wang and Chen.[16] However, for the superimposition the averaged coordinates of the DM-apo-GroEL structure were used, and the direction of the peptide-induced apical domain rotation was shown to be clockwise about the 7-fold symmetry axis, which is opposite to the ATP-induced apical domain rotation.[16] In our study, using the averaged coordinates of the wild-type apo-GroEL structure, we notice a counter-clockwise rotation in both the ATP as well as the peptide-bound GroEL. This is also the direction of the movement of the apical domains observed in a recent EM paper on the structure of a GroEL-protein substrate complex.[17]

Comparison of the apo-GroEL structures with the DM-GroEL(ATP)$_{14}$ and the GroEL-GroES-(ADP)$_7$ structures

The chaperonin GroEL progresses through several different states in the course of a cycle.

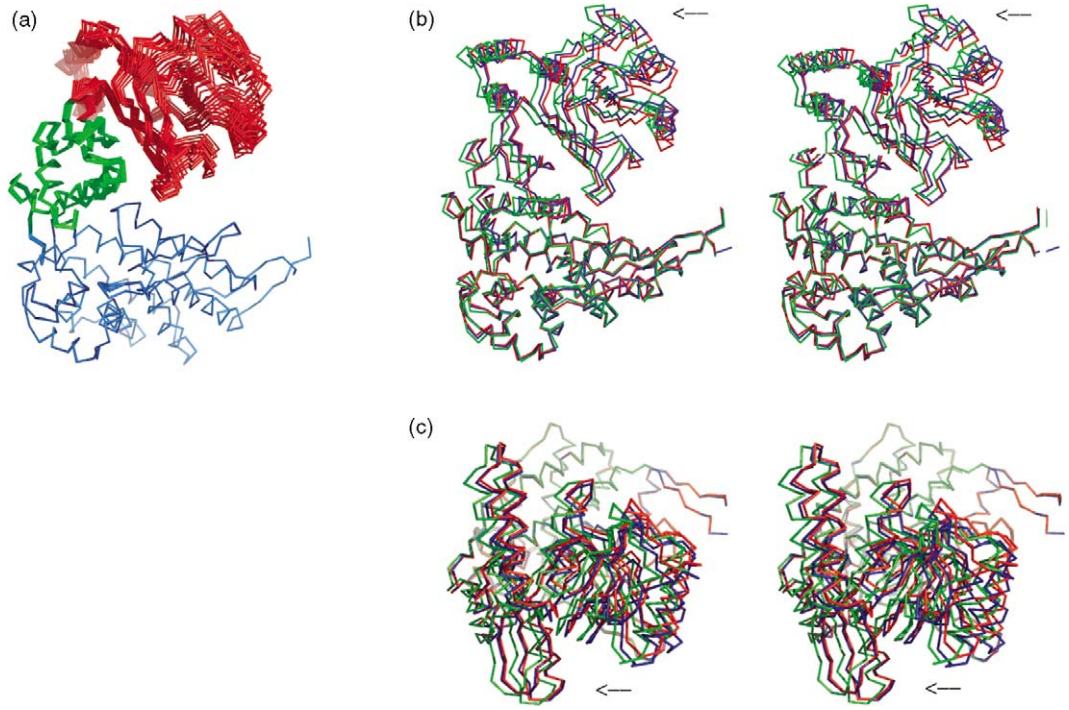

Figure 3. (a) Overlay of all 14 subunits of apo-GroEL showing conformational variability. Equatorial, intermediate and apical domains are colored blue, green and red, respectively. (b) Overlay of the averaged coordinates of the apo-GroEL (red), DM-GroEL-$(ATP)_{14}$ (green), and DM-GroEL(peptide)$_{14}$ (blue) structures. View nearly perpendicular to the 7-fold axis. (c) View along the 7-fold axis. Arrows show the ATP and peptide-induced domain rotation.

Comparison of the available structures at individual stages enables us to deduce through extrapolation the changes undergone by the system during the transition from one step to the next. We compared our structure, representing the "zero state" with the DM-GroEL$(ATP)_{14}$ structure and the structure of the asymmetric complex GroEL-GroES-$(ADP)_7$. The DM-GroEL$(ATP)_{14}$ structure shows no crystallographic symmetry elements relating the protomers in the two rings, and enables us to analyze the involvement of Arg13 in the transmission of the allosteric signal. The ADP-bound asymmetric GroEL-GroES structure of wild-type GroEL represents a later state in the GroEL cycle. Comparison of our structure with this one, provides additional information towards a detailed analysis of the nature of the contacts mediating the cooperativity within and between the rings.

In an effort to further elucidate the mechanism of negative cooperativity, we analyzed our results while keeping in mind two main facts. First, the mutation Arg13Gly causes a dramatic loss of inter-ring communication. Second, binding of ATP and GroES triggers protein folding in the *cis* ring, while in the *trans* ring ATP binding sends allosteric signals to the opposite ring. In addition, in analogy to what has been shown for positive allostery, it can be assumed that the transmission of negative allostery implies alteration of ring–ring interactions. Hence, when comparing the three structures (apo-GroEL, DM-GroEL$(ATP)_{14}$ and GroEL-GroES-$(ADP)_7$), we concentrated on three regions of the equatorial domain: residue 13 and its environment, the ATP-binding site and the ring–ring interface.

The analysis of the structure of another asymmetric complex,[3] GroEL-GroES$(ADP \cdot AlF_3)_7$ (PDB code: 1PCQ) confirmed the observations for GroEL-GroES-$(ADP)_7$. A schematic representation of the interactions observed in the GroEL-GroES$(ADP \cdot AlF_3)_7$ crystal structure is given in Figure S-1 of the Supplementary Data.

Superimposition of the C^{α}-atoms belonging to the equatorial domains of our wild-type apo-GroEL structure on the equivalent ones of either the DM-GroEL$(ATP)_{14}$ structure, or on those of the *trans* ring of the asymmetric GroEL-GroES-$(ADP)_7$ structure, did not show any significant conformational variation of the main chain. However, a detailed analysis of the side-chains revealed many important structural features across the three main selected regions. All possible contacts within these regions were examined. Here we report only the significant differences found among the three structures (Figure 4).

In the apo-GroEL structure the $N^{\eta 2}$ of Arg13 of one subunit is engaged in a salt-bridge with $O^{\varepsilon 2}$ of Glu518 of the same subunit (2.83 Å). There is no interaction of Glu518 with the neighbouring subunit in which $N^{\eta 2}$ of Arg36 is involved in hydrogen bonding with the main-chain carbonyl of Asn457 (2.90 Å), the last residue of helix P (residues 449–457). Through its side-chain ($N^{\eta 2}$) this residue forms also an interaction with the main-chain carbonyls of Lys28 (3.10 Å) and Leu31 (2.90 Å) however, only when the latter is present in the *cis*

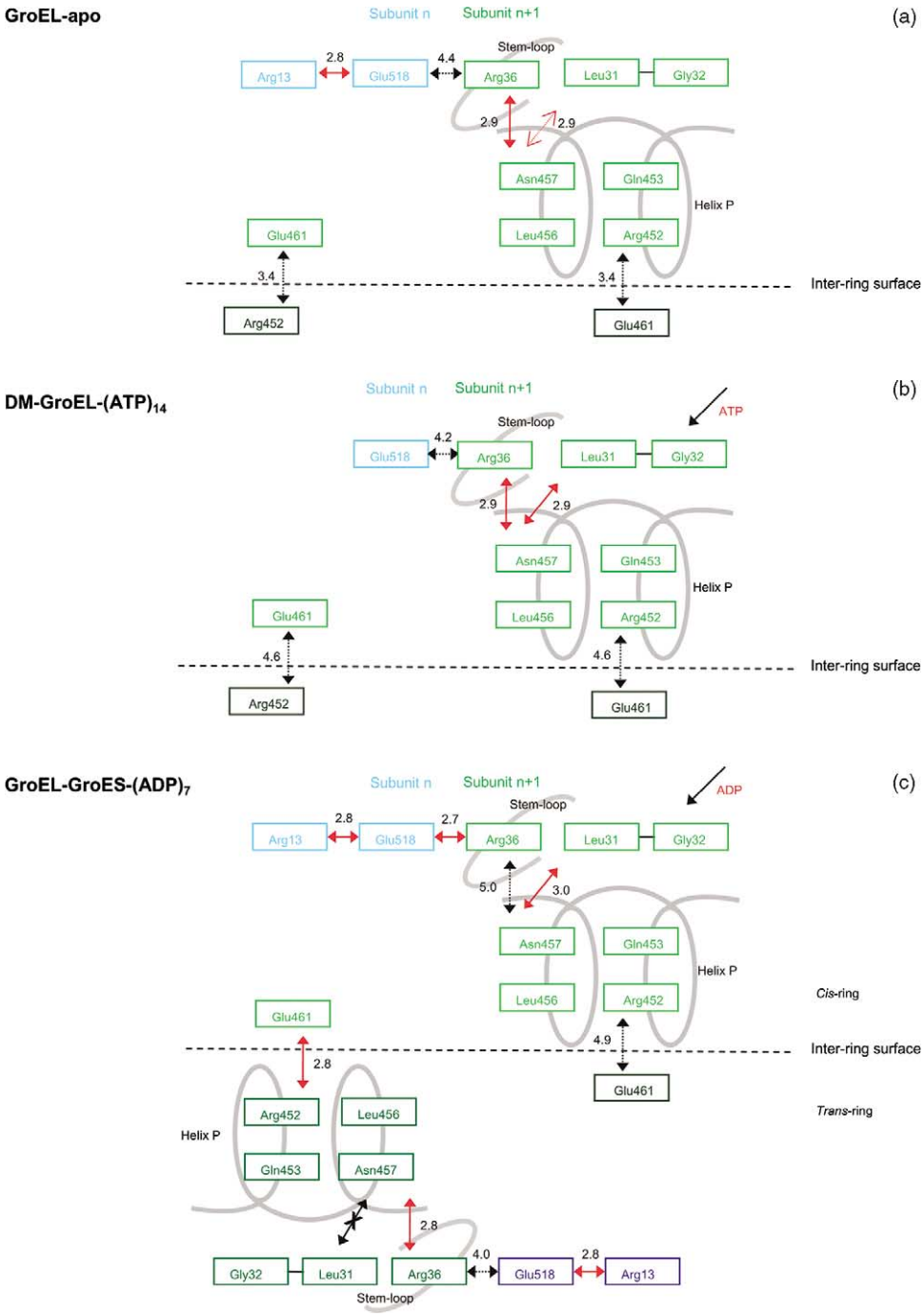

Figure 4. Schematic representation of the interactions observed in three different crystal structures of the chaperonin GroEL. (a) apo-GroEL, (b) DM-GroEL-$(ATP)_{14}$, (c) GroEL-GroES-$(ADP)_7$. The values reported are average distance values. In case of equivalence between the rings (apo-GroEL and DM-GroEL$(ATP)_{14}$) all 14 subunits are considered for averaging, otherwise values are averaged between the seven subunits within each ring (GroEL-GroES-$(ADP)_7$). Full red and dotted black arrows indicate, respectively, the presence or the absence of a salt-bridge; the red dotted arrow in (a) points to the two possible conformations of Leu31, according to which interaction with Asn457 may occur or not. No interaction occurs between Leu31 and Asn457 in the *trans*-ring (c), since Leu31 is present only in the *trans* conformation: this is indicated by a filled black, crossed arrow. The conformation of Leu31 in (b) as well as in the *cis*-ring of (c) is only *cis*. There is no representation for the DM-apo-GroEL structure, since in this case the ring–ring interface results by applying a strict crystallographic 2-fold symmetry. The effect of the Arg13Gly mutation can be extrapolated from (b).

conformation. The two conformations of Leu31 that we observe in the absence of the nucleotide (Figure 1) indicate that in the apo state there is a degree of structural flexibility in that region, the situation that we captured in the crystal structure (flash cooling of the crystals) being one of several. The Arg452 residue, also belonging to helix P, is involved, along with residue Glu461 of the opposing ring, in the main salt-bridge interaction, which stabilizes the association between the two rings: $N^{\eta 2}$

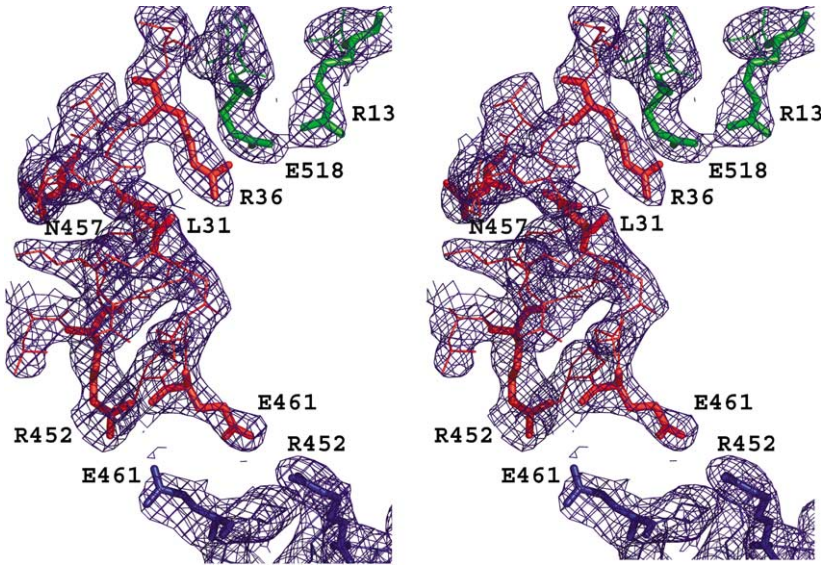

Figure 5. Apo-GroEL structure: the residues involved in the signal path are represented as bold sticks. In green and red are two subunits of one ring; in blue is one subunit of the opposite ring. $2F_o - F_c$ density maps are contoured at 1σ.

of Arg452 and $O^{\varepsilon 2}$ of Glu461 are at an average distance of 3.42 Å (Figures 4(a) and 5).

In the DM-GroEL(ATP)$_{14}$, Glu518 cannot interact with the mutated Arg13Gly. Analogously to the apo structure, Arg36 of a neighboring subunit interacts with Asn457 of the same subunit with an average distance of 2.89 Å. Asn457 interacts also, through its $N^{\delta 2}$, with Leu31 (2.91 Å) whose main chain carbonyl is only found in the "*cis*" conformation (Figure 1). The distance between Arg452 and Glu461 of the opposite ring increases to an average value of 4.60 Å, hence the interface interactions are weakened (Figure 4(b)).

In contrast to the previous two structures, the structure of GroEL-GroES-(ADP)$_7$ is asymmetric and has two dissimilar rings. There is a *cis* and a *trans* ring with very different conformations of both the apical and the intermediate domains while the equatorial domains do not show any dramatic rearrangement in the presence of ADP. There are however small but important differences (Figure 4(c)). The *trans* ring shows great similarities with our apo-GroEL structure: $N^{\eta 2}$ of Arg13 forms a salt-bridge with $O^{\varepsilon 2}$ of Glu518 (2.83 Å); N^{ε} of Arg36 of a neighboring subunit interacts with the carbonyl of Asn457 (2.77 Å). In this ring, the main-chain carbonyl of Leu31 is found only in the *trans* conformation (Figure 4(b)). In the ADP-bound ring there are some rearrangements due to the binding of ADP. $N^{\eta 1}$ of Arg13 still forms a salt-bridge with $O^{\varepsilon 1}$ of Glu518 (2.83 Å), but in this case $O^{\varepsilon 1}$ of Glu518 interacts also with $N^{\eta 1}$ of Arg36 of a neighboring subunit (2.66 Å). This interaction is possible because Arg36 is no longer engaged in a hydrogen bond with $O^{\delta 1}$ of Asn457. In fact $O^{\delta 1}$ of Asn457 is now involved only in the interaction with the carbonyl of Leu31 (3.01 Å), which, analogously to what has been observed in the ADP-bound ring of the GroEL-GroES-(ADP)$_7$ structure, is found only in the *cis* conformation. Examination of the ring–ring interface in this structure shows that the symmetry is broken at the main interaction site: Arg452 in the *trans* ring is engaged in a strong salt-bridge interaction with Glu461 of the *cis* ring with an average distance of 2.80 Å, while the opposite salt-bridge between Arg452 in the *cis* ring and Glu461 in the *trans* ring is strongly weakened with an average distance of 4.93 Å. (Figures 4(c) and 6).

Biological implications

Analysis of the effects of mutations on cooperativity in GroEL contributes to unravel the routes of allosteric communication. It has been shown that positive as well as negative cooperativity are coupled[13,18] and that they can be influenced by mutations distant from the intra- and inter-ring surface,[19,20] however mutations of residues located at contact sites between subunits affect cooperativity too.[7,8,18,21] Specifically the importance of salt-bridges in the allosteric mechanism of cooperative proteins has been acknowledged[22,23] and confirmed

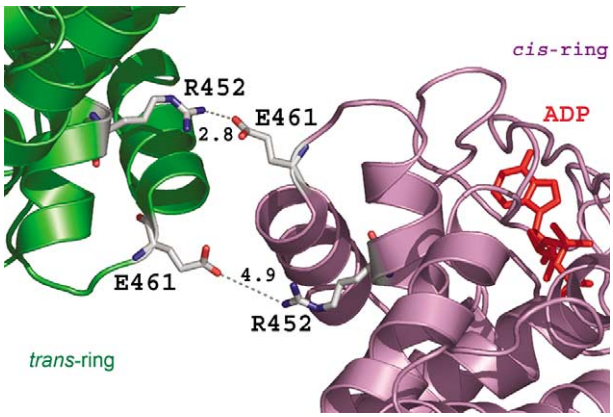

Figure 6. The site of contact at the interface between equatorial domains of the *cis* and the *trans* ring in the GroEL-GroES-(ADP)$_7$ crystal structure. Residues involved in interactions are shown as ball-and-stick models. Salt-bridges are shown as white broken lines.

by site-specific mutagenesis.[8,10,11,13,21] In a recent paper[13] it was also proven that the loss of the salt-bridge Arg452-Glu461, caused by the mutation Glu461Lys is associated with loss of cooperativity in ATP binding and hydrolysis.

The importance of Arg13 has been remarked upon several times, since its mutation to Gly disrupts inter-ring communication. However, Arg13 is not one of the residues located at the inter-ring interface, hence its role must lie in its being part of the signal transmission pathway. Horovitz *et al.*[7] showed that the DM has altered levels of allosteric transitions, which can be understood only by assuming that the two rings become uncoupled as a result of the mutation.

An analysis of correlated mutations in chaperonins[24] aimed at mapping pathways of allosteric communication in GroEL, revealed that Arg13 is a conserved residue across species. In contrast Glu518, located in the equatorial domain, is not conserved. Its mutation has been found to be coupled to that of residue Met267, which is located in the apical domain. A BLAST search revealed that the only mutation occurring at position 518, or its equivalent, within the Cpn60 family is the mutation E518D. It is interesting to notice that this conservative mutation should not alter the binding characteristics of the side-chain, hence keeping intact the capability of forming a salt-bridge.

A further confirmation of the allosteric communication route we hypothesize would come from the analysis of the effects caused by a mutation of Arg36 and of Leu31.

Signal route

According to the GroEL-GroES-$(ADP)_7$ crystal structure, when ATP binds to one subunit, the stem loop (Lys34–Asp52) in the equatorial domain moves allowing for new contacts to be made. In particular the stem loop can now interact with the neighboring helix C (residues 65–85) and with the residues from helix M (residues 386–409) within the same subunit.[5] This stem loop includes Arg36, which, as the comparison of the three structures (apo-GroEL, DM-GroEL$(ATP)_{14}$ and GroEL-GroES-$(ADP)_7$) has shown, plays an important role in the signal communication route that we propose (Figures 6 and 7). Further, it is known[3,5,10] that the α-phosphate of ATP interacts with N of Gly32. This interaction seems to stabilize the *cis* conformation of Leu31, in which the carbonyl group interacts with the $N^{\delta 2}$ of Asn457. In fact in the DM-GroEL$(ATP)_{14}$ structure, as well as in the *cis* ring of the GroEL-GroES-$(ADP)_7$ structure, the *cis* conformation of Leu31 is the only one present. The occurrence of both Leu31 *cis*/*trans* conformations in the apo-GroEL structure points out, that in the absence of the nucleotide a favorable degree of flexibility subsists around this residue.

The interaction of ATP or ADP with Gly32 seems to hinder the rotation of Leu31 by locking the whole group of residues Leu31, Gly32 and Asn457 and extending, through this last residue, the rigidity to the entire helix P. The consequence seems to be a small *en bloc* movement which concerns a large part of the equatorial domain including residues Arg452, as part of helix P, and Glu461, at the C terminus of helix Q (residues 462–471). In fact a 4° *en bloc* inward tilt of the equatorial domains was pointed out in the GroEL-GroES-$(ADP)_7$ structure.[5] We propose that this movement is responsible for the important asymmetry found for the only strong interaction present at the ring–ring interface: the salt-bridge between Arg452 and Glu461 (Figure 6).

In conclusion, the binding of ATP causes a small *en bloc* movement of part of the equatorial domain, which has as a consequence an asymmetry at

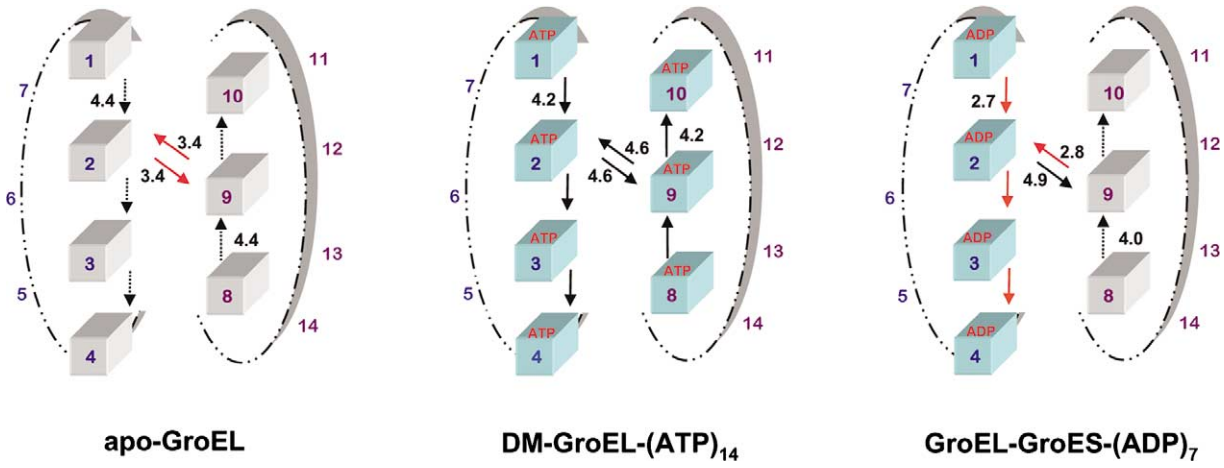

Figure 7. Schematic overview of the interactions between subunits within one ring and between subunits across the ring–ring interface found in the three structures apo-GroEL, GroEL-GroES-$(ADP)_7$ and DM-GroEL$(ATP)_{14}$. Only seven of the 14 subunits are represented with a cube. Red arrows point out the presence of a salt-bridge; black dotted arrows show those contacts, which will give rise to salt-bridges in the course of the cycle; filled black arrows represent those contacts, which, due to the Arg13Gly mutation cannot be involved in salt-bridge interactions. The distances are reported in Å and are the average value of all distances measured within one ring (GroEL-GroES-$(ADP)_7$) or within all 14 subunits of one GroEL molecule (apo-GroEL and DM-GroEL$(ATP)_{14}$).

the ring–ring interface with a strengthening of the salt-bridge Arg452 and Glu461 on one side and weakening on the other side. At the same time, the binding of ATP causes a movement of the stem loop, resulting in the formation of a new salt-bridge between two neighboring subunits of the same ring through the interaction of Arg36 and Glu518. We suggest that these two movements, the *en bloc* inward tilt and the movement of the stem loop, belong to the same signal route, which is shown by the allosteric behavior of the Arg13Gly mutant.

Arg13 and Glu518 are part of a "hinge" at the bottom of two helices, helix A (residues 10–27) and helix R (residues 497–515). The presence of Arg13, engaged in a salt-bridge with Glu518, enables the closure of the hinge: the two helices are locked in their respective position and/or orientation. The Arg13Gly mutation on the other hand, allows the two helices to change this position and/or orientation. As a consequence, even in the presence of ATP, no salt-bridge can be formed between Arg36 and Glu518 (Figure 4(b)) and communication between the two subunits is therefore weakened. This has also an influence on the inward tilt because Arg36, not being engaged in the salt-bridge with Glu518, maintains the interaction with Asn457. Hence, in its stem loop movement, it carries along the whole group of residues Asn457, Leu31, Gly32, helix P and Q with residues Arg452, Glu461. The important consequence is a complete loss of inter-ring communication because the residues responsible for the only salt-bridge present at the ring interface are now at an average distance of 4.6 Å.

Discussion

Throughout the literature on GroEL, reference has been made to the only available non-bound crystal structure, the DM-apo-GroEL structure.[9] However, this has been the source of inaccuracies as it was not clear, to what extent the double mutation created structural deviations from the wild-type structure, but above all, due to the necessity of generating, through crystallographic symmetry, the 14-mer structure. Therefore the consequences of ATP, peptide or GroES binding on the ring–ring interface could not always be analyzed in detail. This is also the case for specific domain motions. Here we provide an apo-GroEL structure, which we consider a more suitable reference structure, since GroEL was obtained from a wild-type strain and there are no crystallographic symmetry elements relating the protomers in the two rings. This new structure allowed us to unambiguously determine the conformation of helix I as well as to confirm the presence of only one strong electrostatic interaction at the ring–ring interface. Furthermore the overlay of all subunits showing a rotational spread of 12.3° at the apical domains, confirmed the mobility of these domains, which confers a high conformational variability to the 14 independent subunits within the oligomer, complying with the ability of the GroEL system to bind different unfolded proteins. According to the maximal rotation angle, the mobility is shown to decrease with the binding of ATP (7.4°) and peptide (2.1°), which is in agreement with the fact that allosteric signals are released upon the binding of both nucleotide and substrate protein. The decrease in mobility in the presence of ATP is similar to what has recently been reported for the eukaryotic cytoplasmic chaperonin containing TCP-1.[25] Overlay of the averaged coordinates of the ATP[10] and peptide-bound[16] GroEL structures with the averaged coordinates of our apo structure also allowed us to confirm that, contrary to what was previously believed, the rotation is always counter-clockwise. This is in agreement with the movement of the apical domains noticed upon binding of a substrate protein.[17]

In their paper Falke and co-workers[17] underline the importance of focusing on the movements between the rings, within the equatorial interface region, which help define the structural elements controlling the negative allosteric effects. Precisely such elements could not be analyzed with the previous DM-apo-GroEL structure, while the study of our apo wild-type GroEL, along with other structures, allowed us not only to do that, but also to suggest a signal pathway, which could contribute to explain the negative cooperativity between the two rings. The proposed mechanism is supported by all biochemical and kinetic studies known so far. We are aware that such a complicated macromolecular arrangement such as GroEL/GroES, involving 14 GroEL and seven GroES subunits, whose interplay with unfolded protein is triggered by ATP, might involve more than one signal route facilitating cooperative action of the subunits within one ring and negative cooperative action of the subunits in the opposite ring. The communication route that we suggest passes through three main points, two of which are situated in neighboring subunits of the same ring and the third in a subunit of the opposite ring (Figures 4 and 7). A signal route of this kind, making use of three points in three separate subunits, has not yet been observed in other multi-subunit assemblies consisting of identical subunits but it answers the question of why a mutation located at a site distant from the ATP binding site can dramatically influence negative inter-ring cooperativity. Exactly such an effect would be expected from the mutation of a residue that is part of a signal transmission route in an allosteric system. In such systems, the regulation of protein function is achieved through conformational changes, induced by binding of substrates or ligands, of parts of the protein that are distant from the binding site.

The participation of the Arg13 in the signal route shows also that communication between neighboring subunits within the nucleotide-bound ring is necessary for transmission of the negative cooperativity signal to the opposite ring. In fact, prevention of such communication is sufficient to reduce

dramatically communication between the rings, as is the case in the DM. The model that we propose therefore reinforces the concept that inter-ring allostery is coupled to intra-ring communication. This is in line with kinetic studies,[26,27] which show that the extent of intra-ring positive cooperativity, with respect to ATP, modulates the rate of inter-ring communication.

Once we realized that the signal transmission involved two subunits within the *cis* ring, we inspected all three structures (apo-GroEL, DM-GroEL(ATP)$_{14}$ and GroEL-GroES-(ADP)$_7$) in order to find evidence of a possible route which, involving Arg13, could influence positive cooperativity. However, we could not find any other possible contribution of Arg13 other than the one described above. This is in accord with kinetic data, which show that positive cooperativity in ATP hydrolysis with respect to ATP, is not affected by the Arg13Gly mutation.[7] The view that other routes are responsible for the transmission of the positive cooperativity signal is supported by several site-specific mutagenesis studies.[8,18] It could be speculated that our suggested three point communication route (Figure 7) is required in order to stabilize the seven-member assembly before the signal is directed to the other ring. Indeed, mutagenesis studies[28] suggest that positive intra-ring cooperativity is required for negative inter-ring allostery, while the reverse is not true, as shown by the DM-GroEL.[7]

In addition to previously reported *en bloc* movements of the equatorial domains, the comparison of the wild-type apo-GroEL structure with the GroEL-GroES-(ADP)$_7$ allowed us to trace movements of single residues which determine whether or not intra-ring as well as inter-ring salt-bridges exist. Examination of such salt-bridges in the asymmetric GroEL-GroES-(ADP)$_7$ crystal structure showed that there are alterations in the ring–ring interface leading to asymmetries in the distances of contacts between corresponding residues in the ADP-bound and ADP-free ring (Figures 4(c) and 6).

Our proposed mechanism for negative cooperativity suggests the coexistence of two types of interactions, similar to those proposed by Ma and co-workers[6] in their model for positive cooperativity, in which structural flexibility as well as electrostatic interactions act in concert and tend to produce a coupled conformational transition. While the major changes occur through *en bloc* movements, minor movements are sufficient to cause the switching of salt-bridges which largely mediate cooperativity in ATP binding. Our results emphasize the primary role of salt-bridges in the propagation of the allosteric signal in the chaperonin system and further validate the view that interactions at contact sites between subunits within the same ring as well as at the interface of two opposing rings, act as points of transmission for allostery.

In the absence of ATP both GroEL rings are in a conformation characterized by low-affinity for ATP. Positive cooperativity in the presence of ATP results in the transition of one ring to a different conformation characterized by high-affinity for ATP, while negative cooperativity hinders the conversion of the opposite ring, thus reaching an asymmetric state.[4] Our study shows that negative cooperativity does not cause an alteration of the conformation around the ATP binding site in the *trans* ring, which resembles the one in the apo-GroEL rings. Conversion of the *trans* ring to a high-affinity state is instead hindered by the introduction of an asymmetry at the ring–ring interface. ATP binding to the *cis* ring causes an increase in the distance of a main inter-ring contact. If this occurred symmetrically in the opposite ring, it would generate an interruption in the inter-ring communication.

In conclusion, we can compare the GroEL system with a three-way switch. The present apo wild-type represents the structure corresponding to the "rest position". The binding of ATP within one ring pushes the switch down on one side and up on the other. In the *cis* ring, the switch is turned on and the conformational changes typical of the folding cycle occur; whereas in the *trans* ring, the switch is turned off and the conformational adaptations taking place are only those required to compensate for the alterations occurring in the *cis* ring and essential to maintain the communication between the rings. This is confirmed by the average distances of the salt-bridge interaction Arg452-Glu461 in the three different structures. In the zero state, the apo structure, the switch is in its resting position (3.42 Å). In the GroEL-GroES-(ADP)$_7$ structure the switch is such that the contact is broken on one side (4.93 Å) while it is strengthened on the other one (2.92 Å). In the DM-GroEL(ATP)$_{14}$ structure, the switch can only be in the "off" position (4.55 Å): no signal can be transmitted through this route and the cooperativity between the two rings is dramatically reduced.

Materials and Methods

Protein expression and purification

Full-length wild-type *E. coli* GroEL was expressed in *E. coli* strain W3110 bearing a multicopy of the non-inducible pOF39 plasmid.[29,30] Cell culture was grown until saturation in rich LB medium to $A_{600\ nm}=3.0$. Cells were collected by centrifugation. Since GroEL was expressed with GroES the two proteins needed to be separated. The cells were disrupted by French Pressure Cell Press (American Instrument Company, USA) in lysis buffer (100 mM Tris–HCl (pH 8.1), 1 mM DTT, 0.1 mM EDTA, 3 mg/ml lysozyme, 0.2 mg/ml PMSF). Cell debris was removed by centrifugation (30,000*g*, 1 h at 4 °C). Cleared lysate was loaded on an ion-exchange DE52-Servacel (Serva) column equilibrated with 30 mM Tris–HCl (pH 7.8), 50 mM NaCl, 1 mM EDTA, 1 mM DTT and eluted at approximately 320 mM of a NaCl gradient (0–500 mM).[31] GroEL containing fractions were diluted five to sixfold with 50 mM histidine–HCl buffer

(pH 5.6–5.8) in order to decrease salt concentration to 50–100 mM of NaCl and to adjust pH for the next chromatography, which was performed on the same column (DE52-Servacel), equilibrated with 25 mM histidine–HCl (pH 5.7), 1 mM DTT. GroEL was eluted with NaCl gradient (0–500 mM) at 300–400 mM NaCl. Pooled GroEL fractions were supplemented with 400 mM $(NH_4)_2SO_4$ and loaded on an hydrophobic interaction Butyl Sepharose column (Pharmacia), equilibrated with 20 mM K–Mops (pH 7.2), 1 mM DTT and 0.4 M $(NH_4)_2SO_4$. GroEL was eluted with the long gradient (400 mM $(NH_4)_2SO_4$–0.0 mM). Eluted GroEL was concentrated either by ultra filtration in a stirring cell (Amicon) and PES membrane (Pall Filtron) with 10 kDa cutoff, or precipitated with $(NH_4)_2SO_4$ before being applied on a gel filtration Sephacryl S-300 column (Pharmacia), equilibrated with storage buffer (30 mM Tris–HCl (pH 7.8), 150 mM NaCl, 1 mM DTT, 0.1 mM EDTA, 0.02% (w/v) NaN_3, 10% (w/v) glycerol). Pooled fractions of oligomeric GroEL were frozen in liquid nitrogen and stored at −80 °C.

Crystal structure determination

Suitable crystals were obtained by the sitting-drop vapour-diffusion method. The well solution contained 100 mM Na-Hepes (pH 7.5), 20% (w/v) PEG 4000, 200 mM $(NH_4)_2SO_4$. Concentration of protein in a drop, after mixing with an equal volume of precipitant solution, was 15–20 mg/ml. Crystals appeared after one week at 18 °C. Crystals were cryoprotected before flash freezing at 100 K with 30% (v/v) of MPD in the mother liquor. A data set was measured to 2.9 Å on a MarCCD at beamline BW6 at DESY-Hamburg and was indexed, integrated and scaled with DENZO and SCALEPACK.[32] Crystal parameters, data collection and processing statistics are given in Table 1. We determined the crystal structure of apo-GroEl with the molecular replacement technique using the DM-GroEL (PDB code 1OEL) as a search model, after removal of all solvent molecules. The original model was stripped back to a poly(Ala) chain and data up to 6.0 Å resolution were used. Two rotation and translation function solutions were identified using the program AMoRe[33] with a cumulative correlation coefficient and R factor of 0.80 and 0.35, respectively. The first noise peak had a cumulative correlation coefficient and R factor of 0.59 and 0.48, respectively. The R factor to 2.92 Å after rigid body refinement was 0.36. All in all 42 rigid body domains: (2×(3(apical, intermediate and equatorial domains)×7)) were considered in order to allow relative domain movements. The model was refined using CNS[34] and 7-fold NCS symmetry restrains were carefully applied. Furthermore, following an established protocol,[11] different weights were carefully chosen to account for the different mobility of the three GroEL domains and of their respective B-factors. Maximum-likelihood simulated annealing using the CNS torsion angle dynamics protocol was carried out.[35] Only variations in the model that resulted in similar decreases in both R factor and R_{free} after refinement were implemented. Furthermore, model building validation during the refinement made thorough use of composite omit SA σ_a-weighted $(2F_o-F_c, \phi_c)$ and (F_o-F_c, ϕ_c) electron density maps. Solvent molecules were added in the latest stages of refinement using the CNS *Water_Pick* utility only if, after visual inspection, positive peaks were: (i) present in both the $2F_o-F_c>1.5\sigma$ and F_o-F_c density maps $>3.0\sigma$; (ii) located within hydrogen bonding distance to a donor or acceptor and (iii) with a temperature factor <80 Å^2 after refinement. Sulfate anions, potassium cations and MPD molecules were manually edited in the electron density maps. Repeated interactions between manual rebuilding and minimization as well as B factor refinement finally resulted in a model that converged to R-factor of 0.20 and R_{free} of 0.24. A summary of the refinement statistics and the stereochemistry analysis is given in Table 1.

Table 1. Crystal parameters, data collection, processing and refinement statistics

Data collection and processing	
X-ray source	BW6/DORIS,DESY, Hamburg
Wavelength (Å)	1.072
Detector	MarCCD
Space group	$P2_12_12_1$
Unit-cell parameters	
a (Å)	262.80
b (Å)	283.60
c (Å)	135.73
Mosaicity (deg.)	0.6°
Resolution range (Å)	33.71–2.92 (3.0–2.92)
No. of measurements	7,717,544
No. of observed reflection $I\geq 0$	374,890
No. of unique reflections $I\geq 0$	184,155 (4965)
Completeness (%)	83.8 (27.4)
Redundancy	1.7 (0.4)
$\langle I/\sigma\ (I)\rangle$ of measured data	11.5 (1.5)
R_{sym}[a] (%)	4.1 (15.8)
Refinement	
Resolution range	33.71–2.92 (Å)
Number of atoms	
Non-hydrogen protein atoms	53,970
Water	847
Non-hydrogen ion atoms (sulfate)	215
Non-hydrogen buffer atoms (MPD)	248
Non-hydrogen PEG atoms	7
Potassium ions	14
R_{crys} (%)	20.3
R_{free} (%)[b]	23.5
r.m.s. deviations from ideal geometry	
Bond lengths (Å)[c]	0.008
Bond angles (deg.)[c]	1.3
Average isotropic B factors (Å^2)	
Equatorial domain (residues 2–136 and 410–525)	32.8
Intermediate domain (residues 137–188 and 378–409)	50.5
Apical domain (residues 189–377)	68.7
Water molecules	28.6
Ions (sulfate)	123.5
MPD	66.1
PEG	87.4
Potassium ions	80.2

Values in parentheses are for the highest resolution shell.

[a] $R_{sym}(I)=\sum_{hkl}\sum_i|I_{hkl,i}-\langle I_{hkl}\rangle|/\sum_{hkl}\sum_i|I_{hkl,i}|$ with $\langle I_{hkl}\rangle$ mean intensity of the multiple $I_{hkl,i}$ observations from symmetry-related reflections.

[b] R_{free} was calculated randomly omitting 10% of the observed reflections from refinement and R-factor calculation.

[c] Stereochemical criteria are those of Engh and Huber.[36]

Figures

Figures were prepared using the program PYMOL (DeLano W.L., The PyMOL Molecular Graphics System. DeLano Scientific LLC, San Carlos, CA, USA†).

† http://www.pymol.org

Protein Data Bank accession codes

Coordinates and structural factors amplitudes have been deposited in the RCSB PDB under the accession code 1XCK.

Acknowledgements

H.H. is grateful for support from DFG grant He1285/13-1. This project has benefitted from the activities of EU-funded DLAB project under contracts HPRI-CT-2001-50035, RII3-CT-2003-505925.

Supplementary Data

Supplementary data associated with this article can be found, in the online version, at doi:10.1016/j.jmb.2005.09.096

References

1. Weber, F., Keppel, F., Georgopoulos, C., Hayer-Hartl, M. & Hartl, U. (1998). The oligomeric structure of GroEL/GroES is required for biologically significant chaperonin function in protein folding. *Nature Struct. Biol.* **5**, 977–985.
2. Grallert, H. & Buchner, J. (2001). Review: a structural view of the GroEL chaperon cycle. *J. Struct. Biol.* **135**, 95–103.
3. Chaudhry, C., Farr, G. W., Todd, M. J., Rye, H. S., Brünger, A. T., Adams, P. D. *et al*. (2003). Role of the γ-phosphate of ATP triggering protein folding by GroEL-GroES: function, structure and energetics. *EMBO J.* **22**, 4877–4887.
4. Horovitz, A., Fridmann, Y., Kafri, G. & Yifrach, O. (2001). Review: allostery in chaperonins. *J. Struct. Biol.* **135**, 104–114.
5. Xu, Z., Horwich, A. L. & Sigler, P. B. (1997). The crystal structure of the asymmetric GroEL-GroES-$(ADP)_7$ chaperonin complex. *Nature*, **388**, 741–750.
6. Ma, J., Sigler, P. B., Hu, Z. & Karplus, M. (2000). A dynamic model for the allosteric mechanism of GroEL. *J. Mol. Biol.* **302**, 303–313.
7. Aharoni, A. & Horovitz, A. (1996). Inter-ring communication is disrupted in the GroEL mutant Arg13→Gly; Ala126→Val with known crystal structure. *J. Mol. Biol.* **258**, 732–735.
8. Ranson, N. A., Farr, G. W., Roseman, A. M., Gowen, B., Fenton, W. A., Horwich, A. L. & Saibil, H. R. (2001). ATP-bound states of GroEL captured by cryo-electron microscopy. *Cell*, **107**, 869–879.
9. Braig, K., Otwinowski, Z., Hegde, R., Boisvert, D. C., Joachimiak, A., Horwich, A. L. & Sigler, P. B. (1994). The crystal structure of the bacterial chaperonin GroEL at 2.8 Å. *Nature*, **371**, 578–586.
10. Wang, J. & Boisvert, D. C. (2003). Structural basis for GroEL-assisted protein folding from the crystal structure of $(GroEL\text{-}KMgATP)_{14}$ at 2.0 Å resolution. *J. Mol. Biol.* **327**, 843–855.
11. Braig, K., Adams, P. D. & Brünger, A. T. (1995). Conformational variability in the refined structure of the chaperonin GroEL at 2.8 Å resolution. *Nature Struct. Biol.* **2**, 1083–1094.
12. Viitanen, P. V., Lubben, T. H., Reed, J., Goloubinoff, P., O'Keefe, D. P. & Lorimer, H. L. (1990). Chaperonin-facilitated refolding of ribulosebiphosphate carboxylase and ATP hydrolysis by chaperonin 60 (GroEL) are K^+ dependent. *Biochemistry*, **29**, 5665–5671.
13. Sewell, B. T., Best, R. B., Chen, S., Roseman, A. M., Farr, G. W., Horwich, A. L. & Saibil, H. R. (2004). A mutant chaperonin with rearranged inter-ring electrostatic contacts and temperature-sensitive dissociation. *Nature Struct. Mol. Biol.* **11**, 1128–1133.
14. Roseman, A. M., Shaoxia, C., White, H., Braig, K. & Saibil, H. R. (1996). The Chaperonin ATPase cycle: mechanism of allosteric switching and movements of substrate-binding domains in GroEL. *Cell*, **87**, 241–251.
15. Sot, B., Galan, A., Valpuesta, J. M., Bertrand, S. & Muga, A. (2002). Salt bridges at the inter-ring interface regulate the thermostat of GroEL. *J. Biol. Chem.* **277**, 34024–34029.
16. Wang, J. & Chen, L. (2003). Domain motions in GroEL upon binding of an oligopeptide. *J. Mol. Biol.* **334**, 489–499.
17. Falke, O., Tama, F., Brooks, C. L., III, Gogol, E. P. & Fisher, M. T. (2005). The 13 Å structure of a chaperonin GroEL-protein substrate complex by cryo-electron microscopy. *J. Mol. Biol.* **348**, 219–230.
18. Yifrach, O. & Horovitz, A. (1994). Two lines of allosteric communication in the oligomeric chaperonin GroEL are revealed by the single mutation Arg196→Ala. *J. Mol. Biol.* **243**, 397–401.
19. Jones, S., Wallington, E. J., George, R. & Lund, P. A. (1998). An arginine residue (Arg101), which is conserved in many GroEL homologues, is required for interactions between the two heptameric rings. *J. Mol. Biol.* **282**, 789–800.
20. Danziger, O., Rivenzon-Segal, D., Wolf, S. G. & Horovitz, A. (2003). Conversion of the allosteric transition of GroEL from concerted to sequential by the single mutation Asp-155→Ala. *Proc. Natl Acad. Sci. USA*, **100**, 13797–13802.
21. Yifrach, O. & Horovitz, A. (1996). Allosteric control by ATP of non-folded protein binding to GroEL. *J. Mol. Biol.* **255**, 356–361.
22. Horovitz, A., Serrano, L., Avron, B., Bycroft, M. & Fersht, A. R. (1990). Strength and co-operativity of contributions of surface salt bridges to protein stability. *J. Mol. Biol.* **216**, 1031–1444.
23. Kantrowitz, E. R. & Lipscomb, W. N. (1990). *Escherichia coli* aspartate transcarbamoylase: the molecular basis for a concerted allosteric transition. *Trends Biochem. Sci.* **15**, 53–59.
24. Kass, I. & Horovitz, A. (2002). Mapping pathways of allosteric communication in GroEL by analysis of correlated mutations. *Proteins: Struct. Funct. Genet.* **48**, 611–617.
25. Rivenzon-Segal, D., Wolf, S. G., Shimon, L., Willison, K. R. & Horovitz, A. (2005). Sequential ATP-induced allosteric transitions of the cytoplasmic chaperonin containing TCP-1 revealed by EM analysis. *Nature Struct. Mol. Biol.* **12**, 233–237.
26. Yifrach, O. & Horovitz, A. (2000). Coupling between protein folding and allostery in the GroEL chaperonin system. *Proc. Natl Acad. Sci. USA*, **97**, 1521–1524.
27. Amir, A. & Horovitz, A. (2004). Kinetic analysis of ATP-dependent inter-ring communication in GroEL. *J. Mol. Biol.* **338**, 979–988.
28. Shiseki, K., Murai, N., Motojima, F., Hisabori, T., Yoshida, M. & Taguchi, H. (2001). Synchronized

domain-opening motion of GroEL is essential for communication between the two rings. *J. Biol. Chem.* **276**, 11335–11338.
29. Fayet, O., Louarn, J. M. & Georgopoulos, C. (1986). Suppression of the *Escherichia coli dnaA46* mutation by amplification of the *GroES* and *GroEL* genes. *Mol. Gen. Genet.* **202**, 435–445.
30. Fayet, O., Ziegelhoffer, T. & Georgopoulos, C. (1989). The *GroES* and *GroEL* heat shock gene product of *Escherichia coli* are essential for bacterial growth at all temperatures. *J. Bacteriol.* **171**, 1379–1385.
31. Harris, J. R., Plückthun, A. & Zahn, B. (1994). Transmission electron microscopy of GroEL, GroES, and symmetrical GroEL/ES complex. *J. Struct. Biol.* **112**, 216–230.
32. Otwinowski, Z. & Minor, W. (1997). Processing of X-ray diffraction data collected in oscillation mode. *Methods Enzymol.* **276**, 307–326.
33. Navaza, J. (1994). AMoRe: an automated package for molecular replacement. *Acta Crystallog. sect. A*, **50**, 157–163.
34. Brünger, A. T., Adam, P. D., Clore, G. M., Delano, W. L., Gros, P., Grosse-Kunstleve, R. W. *et al.* (1998). Crystallography and NMR system (CNS): a new software suite for macromolecular structure determination. *Acta Crystallog. sect. D*, **54**, 905–921.
35. Rice, L. M. & Brünger, A. T. (1994). Torsion angle dynamics: reduced variable conformational sampling enhances crystallographic structure refinement. *Proteins: Struct. Funct. Genet.* **19**, 277–290.
36. Engh, R. A. & Huber, R. (1991). Accurate bond and angle parameters for X-ray protein structure refinement. *Acta Crystallog. sect. A*, **47**, 392–400.

Edited by R. Huber

(Received 31 August 2005; received in revised form 28 September 2005; accepted 29 September 2005)
Available online 21 October 2005